Growth and Anneals of $HgBa_2CuO_{4+\delta}$

UROP Final Report

University of Minnesota (Physics and Astronomy)

Jack Zwettler

September 30, 2019

Abstract

High temperature superconductivity is a phenomenon that exhibits considerable promise in the advancement of technology. The alluring premise of zero resistance at manageable temperatures offers unparalleled minimization of power loss, which necessitates extensive research to aid in understanding the operation of HTSCs (High Temperature Superconductors). This study focused on the well-known HTSC $HgBa_2CuO_{4+\delta}$ (Hg1201). Specifically, the growth procedure was modified using liquid Hg in an attempt to improve crystal quality and size. The frequency of high-quality crystals increased following the change to include liquid mercury in the growth. Additionally, several large crystals were isolated in a higher frequency than with the old growth method. It was also the objective to perform carefully monitored anneals of Hg1201 crystals to modify their oxygen content, with an emphasis on low doping. This was done in order to obtain samples for relevant future experiments. Four anneals were carried out: one highly reduced anneal, two lightly reduced anneals, and one oxidized anneal. These trials yielded inconsistent results.

Overview

As it pertains to research involving Hg1201 crystals, it is often desirable or necessary to have large and relatively high-quality crystals.[1] While such crystals have been observed, the established growth method yields such samples rather infrequently. It is hoped that modifying the growth protocol will yield good samples more often.

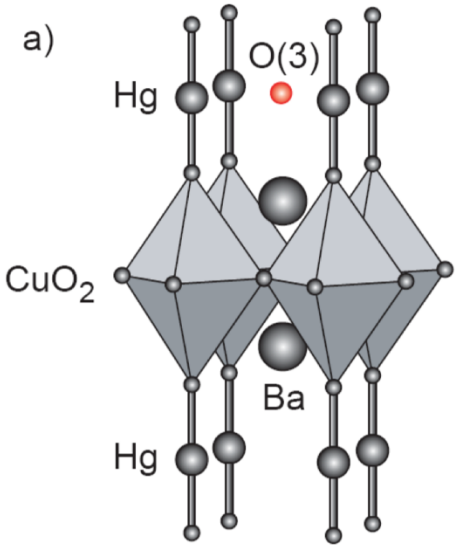

Figure 1: Schematic of the crystal structure of $HgBa_2CuO_{4+\delta}$

Hg1201 is the simplest member of the HTSC $HgBa_2Ca_{n-1}Cu_nO_{2n+2+\delta}$ family, where n = 1. This gives rise to a crystal structure composed of distinct CuO and HgO layers as seen in Figure 1.[1] In the context of superconductivity and other electronic phenomena, the CuO_2 plane is the active layer, which is consistent in other cuprate superconductors.[2] Within this plane, the charge carrier concentration *p*, in the form of holes, controls which electronic states preside in the material at different temperatures.[2] This relationship is displayed in the hole doping-temperature phase diagram in Figure 2.[3] These electronic states are central in experimentation intended to

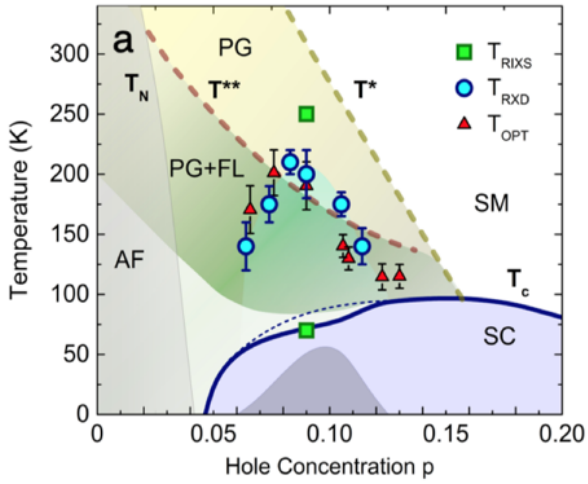

Figure 2: Hg1201 phase diagram. The superconducting transition temperature, T_c, is represented by the solid blue line surrounding the superconducting dome.

aid in understanding the complexity of high temperature superconductivity. Such research efforts include, for example, investigation into Kohler's Rule in magnetoresistance, charge localization, and temperature dependence of resistivity.[4,5,6]

Hole doping can be achieved with relative precision in Hg1201 by means of manipulating the content of interstitial oxygen, shown as the red circle in Figure 1. This doping method is particularly appropriate for this HTSC considering the relatively sizable distance between the aforementioned HgO and CuO layers. Because the HgO layer contains the doped oxygen atom, its disorder effects are minimized with respect to the superconducting CuO layer.[1] As a result, introduced oxygen does not destroy the superconducting phase of the crystal. By annealing as-grown crystals (75 K < T_c < 85 K) over an appropriate duration under a certain oxygen partial pressure, the crystals' hole concentration can be altered. There is great scientific interest in producing highly reduced, or underdoped, crystals of Hg1201 in order to expand the experimental phase diagram and compare with other underdoped cuprates. Highly underdoped crystals with T_c well below 50 K and with hole concentrations below p = 0.06 are somewhat difficult to produce, however, which explains the focus of this project on underdoped anneals.

Growths of $HgBa_2CuO_{4+\delta}$

Prior to this project, all growths followed a specified procedure that consistently yielded crystals of masses of 20-30 mg that were of decent quality. Larger crystals were also produced, but with a much lower frequency. This process was as follows: dry CuO (6.5750 g) and $Ba(NO_3)_2$ (43.2000 g) were mixed and ground finely into a powder. This powder was then placed in a large crucible within a quartz kettle that was then placed within a furnace. Reaching a maximum temperature of 920 ºC, the mixture would form a Ba-Cu-O precursor. The purpose of the quartz kettle was to facilitate constant oxygen inflow as the materials reacted. After around

sixteen hours, this precursor would be abruptly removed and placed in a nitrogen-filled glovebox along with HgO to prevent decomposition. Within the glovebox, 2.1400 g of the precursor, ground moderately before measuring, would be measured as well as 1.5000 g of Hg. It should be mentioned that the scales used had an error of about 0.0005 g, although some past growths succeeded with HgO and/or precursor deficiencies of 2-3 mg. This implies that the sensitivity of the scale did not play a major role in consistency of growths.

In continuing with the growth process, 0.0500 g of Magnesium Sulfate Heptahydrate would be placed with the HgO into the bottom of a quartz tube. The added $MgSO_4$ permitted reasonably sized crystals to form through the release of water into the growth container, which results in larger crystals at the expense of slightly decreased crystal quality. The amount of 50 milligrams was the result of observations of growths over the course of a few months and optimization of the crystal size and quality. Of these growths, $MgSO_4$ deficiencies resulted in crystals that were far too small to be efficiently extracted and measured, and excesses of $MgSO_4$ produced poor-quality crystals that were fragile.

With the $MgSO_4$ and the HgO in the quartz tube, a zirconia crucible containing the precursor would likewise be placed in the quartz tube, which was then sealed under vacuum using a welded quartz plug. After cutting off excess quartz, the tube would be placed into a furnace and heated according to a program that stimulated solid state reactions and crystallization. At the program's completion after roughly five days, the contents of the zirconia crucible would be extracted and picked through, with harvested crystals being stored in Fluorinert FC-40, an inert oil, to prevent decomposition.

Concurrently in the lab, growths of Hg1201's close relative Hg1212 ($HgBa_2CaCu_2O_{6+\delta}$) were improved dramatically with the inclusion of liquid Hg in the growth process. Explosions

due to excess pressure in the sealed quartz tubes during the growth in the furnace became less common as Hg contributes fewer atoms of gas than does HgO in equivalent molar amounts. Additionally, limiting the partial pressure of O_2 (produced from the HgO) was seen to aid in separating the crystals from the growth byproducts. The end result was crystals of higher quality that were produced more consistently.

In consideration of this development, it was decided to add liquid Hg to Hg1201 growths to improve the crystals produced (with the Hg added to the quartz tube at the same time as the HgO). Two different approaches were conducted: Approach 1 replaced a certain amount of HgO with Hg so that the molar amount of Hg remained constant, while Approach 2 introduced Hg and HgO in a manner that would keep the pressure within the quartz tube roughly constant at high temperatures. The details of the first approach are shown in Table 1. With small additions of

Crystal	Precursor mass (g)	Hg (g)	HgO (g)	MgSO4 (g)	Failure?	Additional notes	Date
JZ83	2.1401	0.1007	1.3912	0.0501	No		7-Jun
JZ84	2.1403	0.0987	1.3933	0.0496	Yes: bad weld		7-Jun
JZ85	2.1401	0.1013	1.3906	0.0501	No	Some crystals used in anneal 2019_23 (Also one large crystal of 97 mg was produced)	14-Jun
JZ86	2.14	0.0988	1.3933	0.0502	No	Crystal quality was not ideal	14-Jun
JZ87	2.1401	0.1966	1.2873	0.0502	No	Two very large crystals were produced (140 mg and 87 mg). The former was used in the anneal 2019_27 and 7 others were used in 2019_25	19-Jun
JZ88	2.1396	0.2036	1.2807	0.0497	No	3 crystals were used in 2019_25	19-Jun
JZ89	2.1402	0.2991	1.1772	0.0496	No	Some crystals used in anneal 2019_28, 2 crystals used in 2019_25	27-Jun
JZ90	2.1404	0.3011	1.1753	0.0503	No	Some crystals used in anneal 2019_28	27-Jun
JZ91	2.1401	0.4066	1.0611	0.0497	No	Some crystals used in anneal 2019_28	3-Jul
JZ92	2.1404	0.3953	1.0734	0.0497	No		3-Jul
JZ93	2.1403	0.5036	0.956	0.0499	Yes: Explosion	Precursor powder was left in the sinter furnace for a day	11-Jul
JZ94	2.1402	0.4965	0.9639	0.0501	Yes: Explosion	Precursor powder was left in the sinter furnace for a day	11-Jul
JZ95	2.1402	0.4953	0.9649	0.0503	Yes: Explosion	Vacuum pump was replaced	19-Jul
JZ96	2.1395	0.4956	0.9646	0.0501	Yes: Explosion	Vacuum pump was replaced	19-Jul
CY65	2.1403	0.494	0.9668	0.05	No		25-Jul
CY66	2.1398	0.5073	0.9526	0.05	Yes: Explosion		25-Jul
JZ97	2.1402	0.5971	0.8551	0.0499	Yes: Explosion		2-Aug
JZ98	2.1398	0.6026	0.8488	0.0499	Yes: Explosion		2-Aug
BK2	2.1401	0.1007	1.3914	0.05	No	Alternative quartz plugs were used (36 mg crystal produced)	9-Aug
BK3	2.1403*	0.0994	1.3929	0.0503	No	Alternative quartz plugs were used	9-Aug
JZ99	2.1396	0.2044	1.279	0.0504	No	Some large crystals were produced (59 mg). Also alternative quartz plugs were used	9-Aug
JZ100	2.1396	0.2016	1.2825	0.0504	No	Alternative quartz plugs were used	9-Aug

*Table 1: Growth data from Approach 1. Amounts labeled with * imply a small material spill.*

liquid Hg (i.e. JZ 85, JZ87, BK2, JZ99), some large crystals were produced, with three exceeding 80 mg. This was a significant development, considering that few single crystals from the prior growth method exceeded 50 mg. However, as the amount of liquid Hg increased in the growths, quartz tube explosions became more common, and fewer large crystals were extracted from the

Crystal	Precursor (g)	Hg (g)	HgO (g)	MgSO4 (g)	Failure?	Additional notes	Date
CY55	2.1408*	0.375	1.2002	0.0498	Yes: Explosion		28-Jun
CY56	2.1397	0.3804	1.1959	0.0498	Yes: Explosion		28-Jun
CY57	2.1403	0.3598	1.2001	0.0499	Yes: Explosion		4-Jul
CY58	2.1396	0.3502	1.2085	0.0502	No	Crystals used in 2019_27 and 2019_28	4-Jul
CY59	2.14	0.4768	1.1023	0.05	Yes: Explosion	Precursor powder was left in the sinter furnace for a day	12-Jul
CY60	2.1398	0.4765	1.103	0.0504	Yes: Explosion	Precursor powder was left in the sinter furnace for a day	12-Jul
CY61	2.1402	0.4797	1.1003	0.05	Yes: Explosion	Vacuum pump was replaced	19-Jul
CY62	2.1397	0.4777	1.1018	0.0503	Yes: Explosion	Vacuum pump was replaced	19-Jul
CY63	2.1403	0.602	1.0984	0.05	Yes: Explosion		25-Jul
CY64	2.1399	0.5983	1.1014	0.0496	Yes: Explosion		25-Jul
CY67	2.1399	0.6879	1.0006	0.0505	Yes: Explosion		2-Aug
CY68	2.1399	0.689	1.0005	0.0505	Yes: Explosion		2-Aug
CY69	2.1398	0.4848	1.0964	0.0501	No	Alternative quartz plugs were used, also the HgO was placed inside the crucible	9-Aug
CY70	2.1402	0.478	1.102	0.0504	No	Alternative quartz plugs were used, also the HgO was placed inside the crucible	9-Aug
CY71	2.1402	0.6046	1.0961	0.05	No	Alternative quartz plugs were used, also the HgO was placed inside the crucible. The furnace failed to reach the correct temperatures.	9-Aug
CY72	2.1401	0.6012	1.0991	0.0503	No	Alternative quartz plugs were used, also the HgO was placed inside the crucible. The furnace failed to reach the correct temperatures.	9-Aug

*Table 2: Growth data from Approach 2. Amounts labeled with * imply a small material spill.*

growths that survived. The former phenomenon is somewhat puzzling given that the total pressure within the quartz tube should have been decreasing with increasing liquid Hg in the growth; however, it is possible that the liquid Hg evaporated more rapidly than the solid HgO and caused the pressure to spike before the gaseous Hg had time to react with the precursor.

Approach 2 was less successful at first: most of the initial growths exploded in the furnace. This is shown in growth data for approach 2 in Table 2. However, late in the project, the decision to place HgO inside of the crucible seemed to allow the growths to survive at a higher

rate. The two that were unaffected by furnace malfunction (CY69 and CY70) seemed to offer good crystals, but they offered limited data. Future growths will experiment with this method further.

Growth Characterization

In order to characterize grown crystals, a Quantum Design, Inc., Magnetic Properties Measurement System (MPMS) was used. Allowing for precise control of temperature (± 0.5 %) and external magnetic field (± 0.01 Oe), the MPMS provides a means to easily measure a given sample's transition into superconductivity.[7] The temperature is tuned using a reserve of liquid helium, which allows for temperatures as low as 1.9 K and as high as 400 K to be reached.[3] This was ideal for measurements within this research endeavor, which were all confined within the temperature range between 10 K and 110 K.

The MPMS uses a Superconducting Quantum Interference Device (SQUID), which enables extremely accurate measurements of the magnetic field produced in a superconducting sample in response to an applied magnetic field. SQUID operation uses two superconductors connected by a junction, seen as the blue component in Figure 3.[8] When the magnetic flux Φ changes, so too does the phase difference φ between the two superconducting wavefunctions.[8] The SQUID configuration additionally yields a relationship between $\frac{d\varphi}{dt}$ and the voltage V as shown in Figure 3.[8] This allows changes in flux to be measured as a voltage

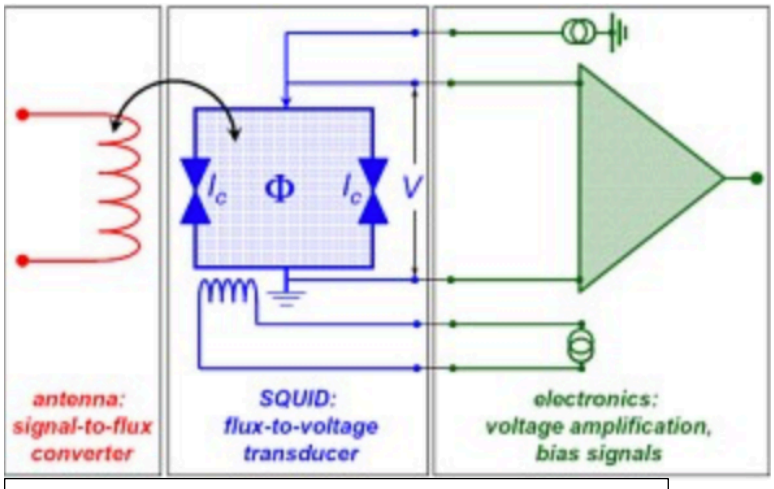

Figure 3: Schematic of a SQUID magnetometer.

difference with great accuracy. In the MPMS, the magnetic signal is obtained through pickup coils as seen in Figure 4.[7] This function is also used to center the crystal for optimal measurements, shown as the location of peak SQUID voltage in Figure 4.[9]

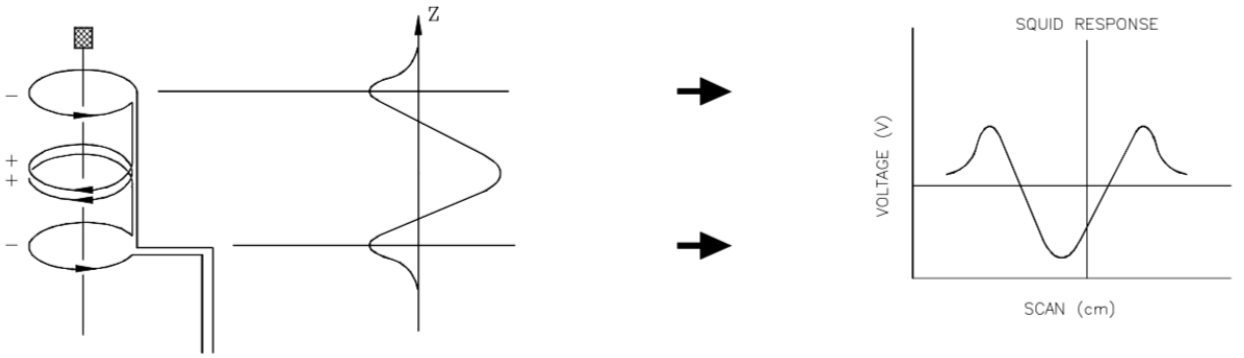

Figure 4: Schematic of MPMS SQUID pickup coils performing a sample measurement

For Hg1201 as-grown crystals, the chosen MPMS program begins by setting the surrounding magnetic field B = 0.00 Oe (1Oe = $1x10^{-4}$ T) to ensure that no magnetic flux can be trapped in impurities within the sample. Also, the temperature is set below the expected transition temperature of the sample. As-grown crystals generally tend to have a T_c between 75 K and 85 K, so a typical value for this lower temperature limit is 65 K or 60 K. The magnetic field is then be set to 5.00 Oe and the temperature is increased beyond the expected transition temperature, normally stopping at 90 K or 95 K. This initial temperature sweep is referred to as a "zero field cooled" sweep (ZFC). Keeping the magnetic field at 5.00 Oe, the program cools down the sample to the lower temperature limit and proceeds through the "field cooled" sweep (FC). During each temperature sweep, the MPMS measures the magnetic field produced by the sample response to the applied field. Ideal superconductors act as perfect diamagnets due to the Meissner-Ochesnefeld effect, whereby magnetic flux is expelled from a superconductor when it

is cooled below T_c. An example of the resulting data is shown in Figure 5. The ratio of the produced field to the applied field (the magnetic susceptibility) should be $\chi = -1$ for an ideal superconductor below its transition temperature. Exploiting this feature enables qualitative measurement of any given sample's quality using the ZFC and FC temperature sweeps. In a perfect superconductor, the minimum measured susceptibility for both sweeps should be the same, so the ratio of field-cooled to zero-filled-cooled magnetic susceptibility, known as the FC/ZFC ratio, is 1. However, the fact that magnetic flux is allowed to remain trapped in the impurities within the sample during cooling in an applied magnetic field (and not during zero-field cooling) manifests as a FC/ZFC ratio that is less than 1. It is therefore the case that poor-quality samples will yield a smaller ratio than higher quality samples.

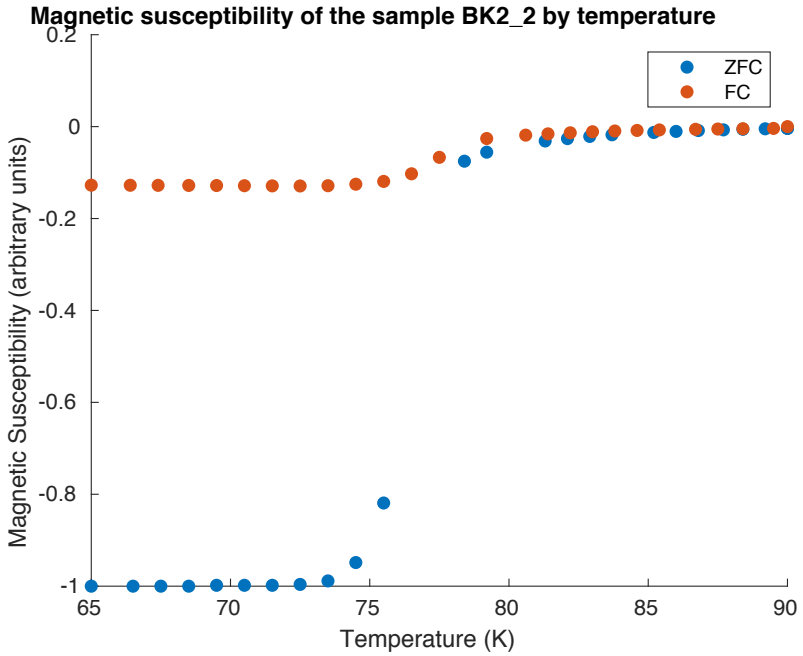

Figure 5: A plot of ZFC and FC temperature sweeps for the Hg1201 sample BK2_2. The magnetic susceptibility values were found by assuming that the value of the produced magnetic field when $T<T_c$ in the ZFC sweep corresponded to a magnetic susceptibility χ = -1, corresponding to a perfect diamagnet.

Data pertaining to crystal characterization is shown in Figure 6 in a comparison between crystals from the liquid Hg growths and crystals from the old method. For as-grown crystals, the

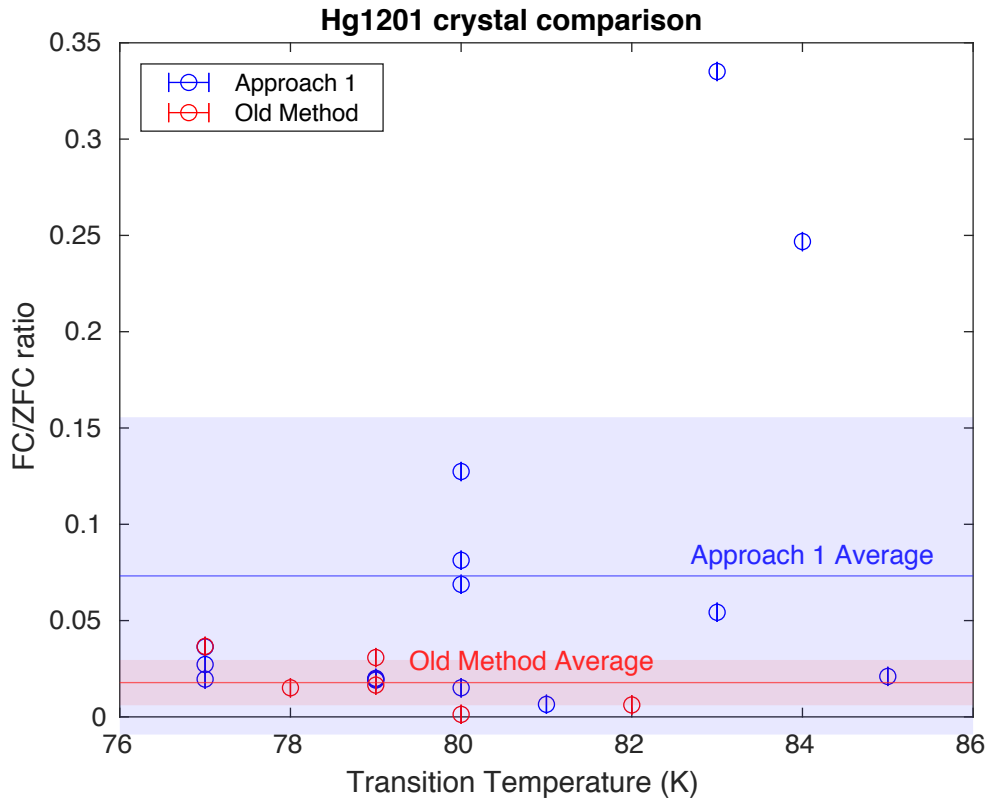

Figure 6: MPMS data for Hg1201 crystals. Data points correspond to an individual crystal's transition temperature and FC/ZFC ratio. The transition temperature was found by taking the average of the 10% and 90% susceptibility values during the temperature transition of the ZFC sweep. The FC/ZFC ratio was the ratio between the smallest measured susceptibility for the FC and ZFC temperature sweeps. Entries in blue correspond to Approach 1, and entries in red correspond to the old growth method. The blue shaded region corresponds to FC/ZFC ratios within one standard deviation of the mean for Approach 1 (solid blue line), and the red shaded region corresponds to FC/ZFC ratios within one standard deviation of the mean for the old method (solid red line). Please note that the FC/ZFC ratio is not necessarily dependent on the transition temperature, and the plot is merely a means of displaying the data.

temperature transition is mostly constant, so it is not of particular interest. However, the crystal quality, conveyed by the FC/ZFC ratio, is very important for such crystals. The data from Figure 6 indicate that the crystal quality may have improved on average with the addition of liquid Hg, but the significance of the enhancement is unclear. However, the frequency of high-quality crystals ostensibly increased, as 6 crystal samples exhibited an FC/ZFC ratio greater than 0.05, which was very uncommon in reasonably sized crystals from the prior growth method.

It should also be noted that the growths producing crystals with the best FC/ZFC ratios (JZ87, BK2, and JZ99) all corresponded to relatively low amounts of liquid Hg. In combination with evidence that these low liquid Hg growths tend to produce larger crystals, it is reasonable to infer that this growth method has the most potential from Approach 1. Future efforts will therefore focus on its optimization.

Anneals of $HgBa_2CuO_{4+\delta}$

Over the course of this project, four anneals were completed. The first, labeled 2019_23, was intended to produce highly underdoped crystals. Composed of ten Hg1201 crystals, this anneal spanned four weeks in constant conditions of a medium vacuum (~5.4 mTorr) at a temperature of 400 ºC. Pressure and temperature readings were monitored daily using a pressure gauge and a thermocouple mounted in the annealing furnace. The crystals were held in a ZrO_2 boat that was placed within a quartz tube. This setup simplified removal of the crystals from the furnace at the anneal's completion, when the crystals were quickly dumped into Fluorinert FC-40 in order to "quench" them and quickly stop the anneal. Data from characterization of this anneal is shown in Table 3. While the transition temperatures of the crystals were quite low, which was an objective of the anneal, they were

2019_23_#			Tc (K) (± 1 K)	FC/ZFC (± 0.0001)	Transition (K) (± 1 K)
1	Erratic measurement		N/A	N/A	N/A
2			31	0.0478	16
3			34	0.1106	7
4			18	0.0195	12
5			25	0.0043	18
6			24	0.0098	20
7			31	0.0306	9
8			28	0.0692	10
9			26	0.0293	9
10			25	0.0337	12
		AVERAGE	27	0.0394	13
		Standard Deviation	5	0.0331	4

Table 3: Characterizations of crystals from 2019_23

also quite inconsistent. Given that all of the crystals should have had approximately the same T_c prior to the anneal and the conditions were constant, this discrepancy is rather unexpected. It is possible that initial sample quality and size affected the outcomes, but this was not observed in the other anneals. Further tests must therefore be conducted in this highly important doping range.

The next anneal, 2019_24, was intended to achieve optimal doping, i.e. the doping level where T_c is maximized at about 97 K for Hg1201. Using past anneals, it was concluded that the treatment should include high oxygen pressure (~4 atm) by means of dissociated AgO (0.3600 g) in an initially evacuated (245 mTorr) quartz tube at 300 ºC for four weeks. The process for preparing this anneal was not unlike normal Hg1201 growths in that the AgO and the crucible containing the crystals were placed in a quartz tube and sealed with a quartz plug. Anneals 2019_25 and 2019_26 were both intended as slightly underdoped anneals with a process similar to 2019_23, except a constant nitrogen gas flow was used in place of the vacuum. The temperatures used were 450 ºC and 400 ºC, respectively. Characterization data from these anneals are shown in Figure 7. From the figure, it is

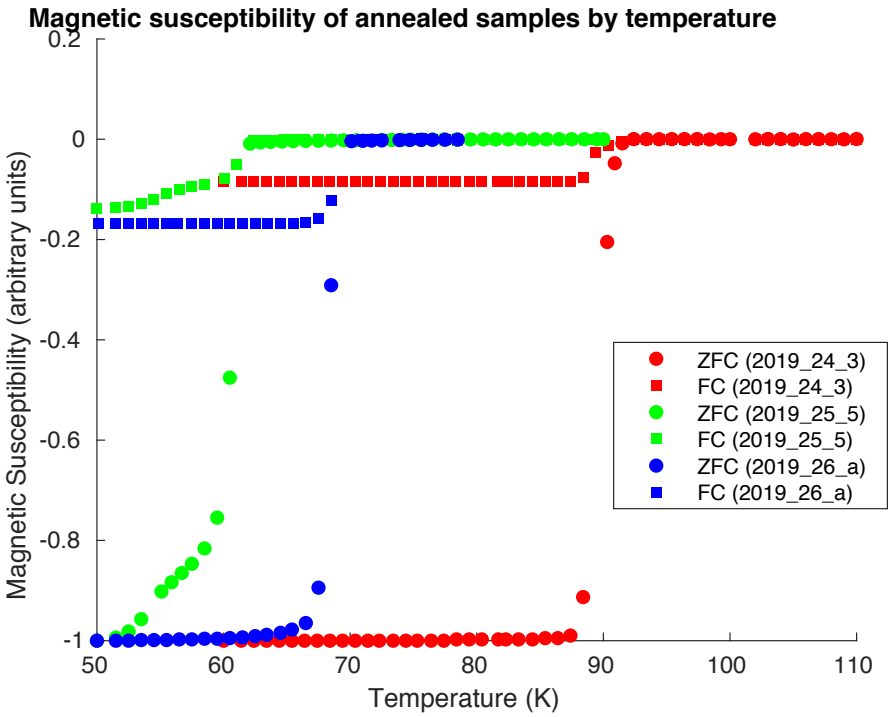

Figure 7: Plots of ZFC and FC temperature sweeps for the samples 2019_24_3, 2019_25_5, and 2019_26_a.

observable that each anneal yielded crystals of decent quality with different transition temperatures. Furthermore, each T_c behaved as expected given the annealing conditions. This is promising for future anneals that are intended to produce lightly underdoped or optimally doped crystals.

Conclusion

Focusing on the HTSC crystal $HgBa_2CuO_{4+\delta}$, efforts from this project resulted in improvement of crystal growth from the original growth strategy. The inclusion of liquid Hg was shown to yield high-quality crystals more frequently and to provide an increased tendency for growths to produce large crystals conducive for further experimentation. Additionally, anneals were carried out for Hg1201 with mixed results. Very low doping continued to present challenges in consistency and quality, while higher doping was achieved relatively successfully. In a cumulative outlook, work with growth and modification of Hg1201 crystals has direction for optimization as a result of the findings from this project. In future research, it is hoped that the subtleties of the mechanisms of high temperature superconductivity are uncovered in $HgBa_2CuO_{4+\delta}$ as well as other HTSC's in the quest for widespread application of such materials.

Acknowledgements

I enjoyed carrying out this research project, and I felt as though the work was extremely fulfilling. I would therefore like to thank those from the Undergraduate Research Opportunities Program that made this work possible. Additionally, I thank Martin Greven for allowing me to participate in his superconductivity lab, as well as other members of the lab in graduate students Zach Anderson and Chiou Yang Tan, undergraduates Zi Wang and Liam Thompson, and Dr. Nikolaos Biniskos, who all assisted me in completing this project.

References

[1] Barišić, N.; Li, Y.; Zhao, Y.; Cho, Y.; Chabot-Couture, G.; Yu, Guichuan; Greven, M. "Demonstrating the model nature of the high-temperature superconductor $HgBa_2CuO_{4+\delta}$." *Physical Review B,* **78**, 054518-20 (2008).

[2] Bernhard, C.; Tallon, J. L. "Thermoelectric power of $Y_{1-x}Ca_xBa_2Cu_3O_{7-\delta}$: Contributions from CuO2 planes and CuO chains." *Physical Review B,* **54**, 10201 (1996).

[3] Yu, B.; Tabis, W.; Bialo, I.; Yakhou, F.; Brookes, N.; Anderson, Z.; Tang, Y.; Greven, M. "Unusual dynamic charge-density-wave correlations in $HgBa_2CuO_{4+\delta}$." arXiv:1907.10047 (2019).

[4] Chan, M. K.; Veit, M. J.; Dorow, C. J.; Ge, Y.; Li, Y.; Tabis, W; Tang, Y.; Zhao, X.; Barišić, N.; Greven, M. "In-Plane Magnetoresistance Obeys Kohler's Rule in the Pseudogap Phase of Cuprate Superconductors." *Physical Review Letters*, **113**, 177005 (2014).

[5] Pelc, D.; Popčević, P.; Požek, M.; Greven, M.; Barišić, N. "Unusual behavior of cuprates Explained by heterogeneous charge localization." *Science Advances*, **5**, 1 (2019).

[6] Pelc, D.; Veit, M. J.; Chan, M. K.; Dorow, C. J.; Ge, Y.; Barišić, N.; Greven, M. "The resistivity phase diagram of cuprates revisited." arXiv:1902.00529 (2019).

[7] "Magnetic Property Measurement System – MPMS® - XL." *LOT-Oriel Group Europe*, Quantum Design (2011).

[8] "SQUID Magnetometry." *Walther-Meißner-Institute for Low Temperature Research* (2019).

[9] "MPMS MultiVu Application User's Manual." *Pharos Digital Library*, Quantum Design (2012).